

Photoconductance quantization in a single-photon detector

Hideo Kosaka,^{1,*} Deepak S. Rao,¹ Hans D. Robinson,¹ Prabhakar Bandaru,¹ Toshitsugu Sakamoto,² and Eli Yablonovitch¹

¹Electrical Engineering Department, University of California Los Angeles, Los Angeles, California 90095-1594

²Fundamental Research Laboratories, NEC Corporation, 34 Miyukigaoka, Tsukuba, Ibaraki 305-8501, Japan

(Received 19 December 2001; published 13 May 2002)

We have made a single-photon detector that relies on photoconductive gain in a narrow electron channel in an $\text{Al}_y\text{Ga}_{1-y}\text{As}/\text{GaAs}$ two-dimensional electron gas. Given that the electron channel is one dimensional, the photoinduced conductance has plateaus at multiples of the quantum conductance $2e^2/h$. Superimposed on these broad conductance plateaus are many sharp, small, conductance steps associated with single-photon absorption events that produce individual photocarriers. This is a first step toward a photoconductive detector that could measure a single photon, while safely storing and protecting the spin degree of freedom of its photocarrier, but we have not actually achieved that goal.

DOI: 10.1103/PhysRevB.65.201307

PACS number(s): 72.20.-i, 72.40.+w, 73.63.-b, 78.67.-n

The detection of individual photons has become common in the last few decades with the proliferation of avalanche photodetectors,¹ and negative electron affinity² photocathode photomultipliers. However, it is becoming desirable now to transmit something more sophisticated than single-photon states. Namely, we want to distribute quantum entanglement information over long distances to enable teleportation³ and other forms of advanced telecommunication. For this, single-photon sensitivity is not enough. New types of single-photon photodetectors are needed, which preserve the spin information of the photocarrier.

New selection rules have been identified in the III-V semiconductor photodetectors, which permit the transfer⁴ of photon polarization information directly to photoelectron spin. Unfortunately, the avalanche multiplication process is relatively violent, of necessity, and it destroys any spin information that might have been present on the original photoelectron. New forms of single-photon detection have been developed recently that are gentle enough to preserve the photoelectron spin state, while providing the gain needed to detect a single photon. For example, photoconductive gain can provide for single-photon detection.

Shields *et al.*⁵ recently demonstrated single-photon sensitivity in a two-dimensional (2D) electron channel controlled by photoelectric charge trapped on adjacent $\text{In}_x\text{Ga}_{1-x}\text{As}$ precipitates in $\text{Al}_y\text{Ga}_{1-y}\text{As}$. In photoconductive gain, electric charges become trapped for long periods, and while trapped, their electric charge can influence the channel conductivity. Over time, vast amounts of electric charge can be transferred in the channel current, far more than the original trapped charge, creating a huge photoconductive gain. Trapping of an individual photocarrier produces a step function in current that can persist for long periods. In $\text{Al}_y\text{Ga}_{1-y}\text{As}$ alloys at low temperature this is called persistent photoconductivity, and the current can last for weeks. An analogous electrical transport sensitivity enhancement was spectacularly used to detect individual far-infrared photons by Komiyama *et al.*⁶

In this report, we demonstrate that an ordinary, conventional, $\text{Al}_y\text{Ga}_{1-y}\text{As}/\text{GaAs}$ modulation-doped field effect transistor, in a 2D electron gas (2DEG) quantum point contact configuration, can already detect single-photon events. $\text{In}_x\text{Ga}_{1-x}\text{As}$ precipitates in GaAs are unnecessary, as the ordinary defect centers that are already present in

$\text{Al}_y\text{Ga}_{1-y}\text{As}/\text{GaAs}$ can trap photocarriers successfully. Furthermore, the trapped photocharge has the same effect as a positive external gate in unpinching the channel, leading to conductance quantization steps. Thus we are in the interesting situation where individual single-photon-conductivity steps are superimposed on the one-dimensional (1D) channel conductance quantization steps associated with a variable width point contact channel. As an aside, this may also be the first observation of photoinduced 1D channel conductance quantization.

The sample used for these experiments is a modulation-doped heterostructure with a quantum point contact defined by a pair of split gates on $\text{Al}_{0.3}\text{Ga}_{0.7}\text{As}/\text{GaAs}$, as illustrated in Fig. 1. All layers are grown by molecular beam epitaxy on semi-insulating GaAs, consisting of a nominally undoped GaAs buffer layer, an *i*- $\text{Al}_{0.3}\text{Ga}_{0.7}\text{As}$ spacer layer 30 nm thick, a Si-doped ($1 \times 10^{18} \text{ cm}^{-3}$) *n*- $\text{Al}_{0.3}\text{Ga}_{0.7}\text{As}$ layer 60 nm thick, and a Si-doped GaAs cap layer, 5 nm. The 2D

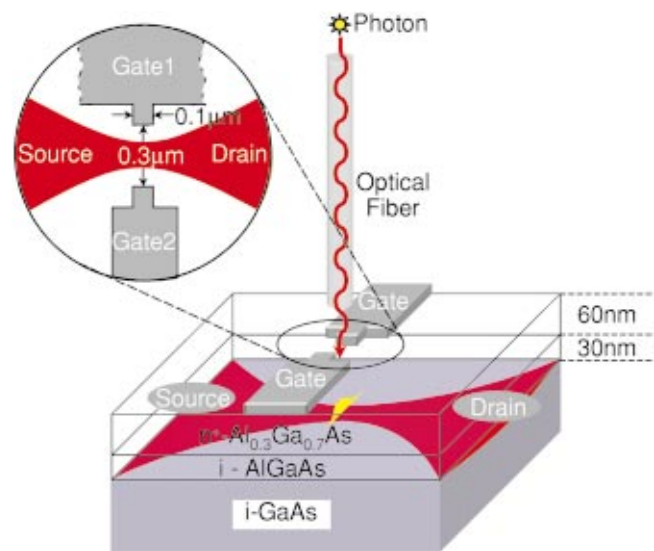


FIG. 1. (Color) Schematic diagram of the experimental setup. A nearly pinched off point contact channel in a 2D electron gas at an $\text{Al}_y\text{Ga}_{1-y}\text{As}/\text{GaAs}$ interface can act as a sensitive photodetector. The source/drain channel conductance can sense individual trapped photocarriers, whose effect is multiplied by the photoconductive gain mechanism.

electron gas in the heterointerface has a carrier density of $3.3 \times 10^{11} \text{ cm}^{-2}$, a mobility of $1.1 \times 10^6 \text{ cm}^2/\text{Vs}$, and a Fermi energy (E_F) of 11.8 meV. The Ti/Au split gate, of lithographic length $0.1 \mu\text{m}$, and spacing $0.3 \mu\text{m}$, is fabricated on the heterostructure using electron-beam lithography and electron-gun evaporation. The 1D channel is formed as a line by depletion in the 2DEG between the two gates.

The sample is illuminated by monochromatic light through a large-core glass fiber, which is carefully shielded to block any photons from the outer jacket. The light is created by a tungsten lamp and then filtered by a monochromator, a long-pass filter passing wavelengths $\lambda > 530 \text{ nm}$, and a 20 dB neutral density filter. The optical power at the end of the fiber measured by a Si detector is $\approx 9 \text{ pW}$. The area of illumination at the device is about 1 mm in diameter due to end-fire coupling from the fiber. Given the small device area $3 \times 10^{-10} \text{ cm}^2$ defined by the gates, we estimate the actual light power in the active area to be 7×10^{-9} times smaller. Thus the incident photon flux is estimated to be 0.1 photon per second on the effective device area.

The source/drain current is measured at a constant voltage drop (V_{SD}) of 0.5 mV, at a temperature of 4.2 K. Figure 2(a) shows the corresponding source/drain conductance, as a function of either gate voltage or of the light exposure time. As the channel is opened up, a series of electron wave-guided modes successively contribute conductance steps,^{7,8} in units of the conductance quantum, $2e^2/h \approx 1/13\,000 \Omega$, where e is the electronic charge, the factor 2 accounts for spin, h is Planck's constant, and Ω is ohms. The first two steps are shown in Fig. 2(a), and their sharpness is consistent with the temperature, 4.2 K. In addition there is a well-known⁹ shoulder at conductance $0.7(2e^2/h)$ thought to be associated with electron spin exchange interaction¹⁰ effects.

What is remarkable about Fig. 2(a) is that there are two different physical phenomena, producing almost identical source/drain conductance on the vertical axis. The curve labeled "gate only" shows that positive gate voltage, above the -1.5 V gate threshold, opens up the electron channels producing conductance steps. Likewise, exposure to a weak light source of wavelength $\lambda = 700 \text{ nm}$ at a fixed bias voltage produces trapped positive charge that also opens up the electron waveguide channels, producing exactly the same conductance steps. In fact the processes are the same. In either case, positive net charge opens up the source/drain electron current channels, leading to the observed electron conductance steps.

An enduring, photoinduced increase in conductivity has been well known^{11–13} in III–V semiconductors, and is called persistent photoconductivity. At temperatures much lower than 100 K the net positive trapped charge is known to persist for weeks. The photoexposure begins at time $t = 0$ in Fig. 2(a), to the right of the crosshatched dark region where the conductivity begins as a constant. If the photoexposure is prematurely terminated, the conductance becomes constant again in Fig. 2(a), persisting at the new value for weeks.

Photoconductivity in an electron channel requires fixed positive charge from trapped photoholes. The hole trapping centers can be either neutral donors d^0 , which become ion-

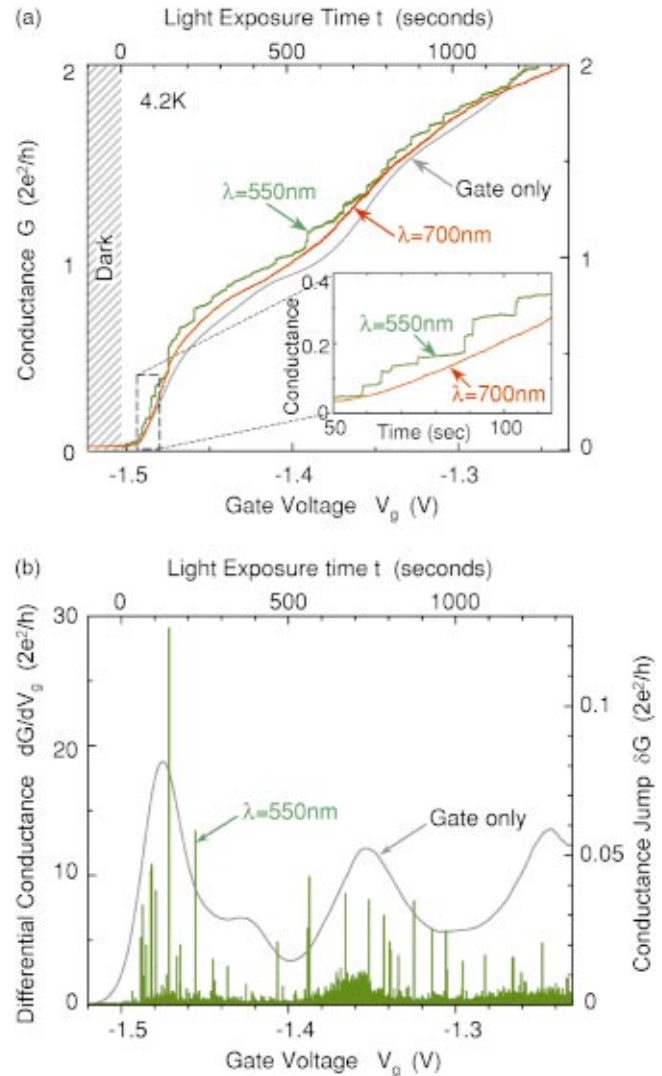


FIG. 2. (Color) (a) The source/drain channel conductance induced by a modulation of a gate voltage, and by light exposure for a period of time. The conductance quantization plateaus at multiples of $2e^2/h$ are practically identical. With light at $\lambda = 550 \text{ nm}$, there is the additional feature of individual small conductance steps associated with single photons. (b) Differential conductance dG/dV_g versus gate voltage, and individual photon conductance jump height versus light exposure. The single-photon conductance jumps are larger at those bias conditions where the channel conductance is more sensitive to gate voltage.

ized undergoing the transition $d^0 + h^+ \rightarrow d^+$, or they can be DX^- centers^{14–18} that become neutralized by hole capture,¹⁹ $DX^- + h^+ \rightarrow d^0$. In any case, the net trapped positive charge has the same effect on the source/drain electron channel as positive gate increments do. The only difference in Fig. 2(a) is that the horizontal axis at the top measures the net positive charge in terms of optical exposure time from a weak $\lambda = 700 \text{ nm}$ beam, and the horizontal axis at the bottom measures positive increase of gate voltage. The same quantum conductance plateaus are produced in either case.

When the photon wavelength is reduced to $\lambda = 550 \text{ nm}$, well beyond the $\text{Al}_{0.3}\text{Ga}_{0.7}\text{As}$ band gap, an additional phenomenon appears, which is plotted in Fig. 2(a) as the curve

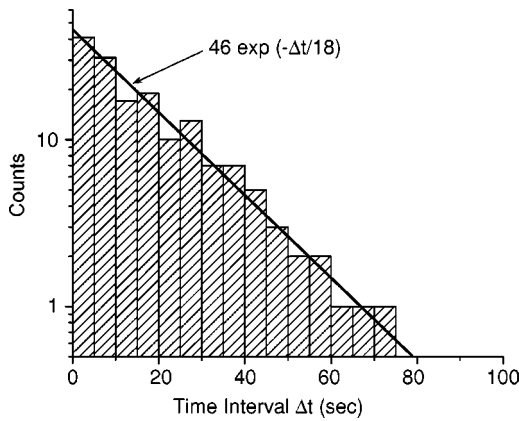


FIG. 3. Statistics of the time intervals between single-photon detection events. The exponential decay is consistent with unsqueezed photon statistics.

labeled “ $\lambda = 550$ nm.” That curve still follows the overall shape of the quantized conductance steps, but the curve itself consists of many smaller steps that, in aggregate, produce the quantized conductance shape, including the $0.7(2e^2/h)$ feature. We attribute the smaller steps, to absorption of individual photons, and the corresponding capture of a single photohole. Since the traps are at variable distances from the source/drain channel, each photon produces a different step height. This is different from the Millikan oil-drop experiment, but similar to the observations by Shields *et al.*,⁵ who trapped photoholes on $\text{In}_x\text{Ga}_{1-x}\text{As}$ islands.

The photon steps for $\lambda = 550$ nm in Figs. 2(a) seem to be taller where the conductance curve is steeper, due to greater sensitivity to electrostatic charge changes when dG/dV_g is larger. This point is illustrated in Fig. 2(b), which plots (1) dG/dV_g versus gate voltage on the left and bottom axes, and on the same graph and (2) δG , single-photon step height versus photon exposure time on the right and top axes, respectively.

The $\lambda = 550$ nm “curve” in Fig. 2(a) is seen in Fig. 2(b) to consist of about 70 individual photon steps. We can test for proper photon statistics by plotting a histogram of the time intervals between photon events, as illustrated in Fig. 3. The intervals should fall on a decaying exponential for random photon events, as is appropriate for unsqueezed photon statistics, with the average interval between photon events being 18 s in this case. This low photon detection rate is consistent with an active area of 3×10^{-10} cm², and a quantum efficiency of around 30%. The monotonic upward conductance changes are to be distinguished from a “random telegraph signal,”²⁰ which fluctuates in either direction.

The wavelength dependence of the onset of the single-photon-conductivity steps is correlated with the 1.9 eV band gap of the $\text{Al}_{0.3}\text{Ga}_{0.7}\text{As}$ layer, on top of the 2D electron gas. The onset of single-photon steps begins at wavelengths shorter than $\lambda < 650$ nm, becoming more pronounced at $\lambda = 550$ nm where the $\text{Al}_{0.3}\text{Ga}_{0.7}\text{As}$ is more absorbing. By contrast, the single-photon steps are not seen at $\lambda = 700$ nm. A corresponding model of the photoconductive process at $\lambda = 550$ nm is illustrated in Fig. 4. A photon is absorbed in the $\text{Al}_{0.3}\text{Ga}_{0.7}\text{As}$ layer, with the photohole being

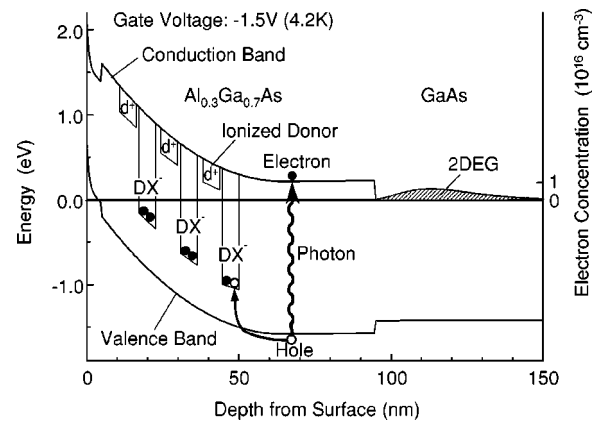


FIG. 4. A model for the single-photon detection, carrier capture, and the photoconductive gain mechanism. A photohole is trapped at either a DX^- center or a neutral donor d^0 . The net positive charge increases the source/drain electron channel conductance. The long-lived electron current passing through the channel over time is responsible for the photoconductive gain mechanism.

trapped at DX^- centers that are associated with the n -type doping. Alternately the photohole can be trapped at neutral donors, d^0 , though none are shown in Fig. 4. (According to the negative- U property²¹ of DX^- centers, neutral donors segregate into ionized donors d^+ and DX^- centers.) Regardless, in either case, the net increase in positive charge among the donor defects opens up the source/drain channel creating a permanent increase in electron current.

Conversely, at $\lambda = 700$ nm, photons are absorbed in the nominally undoped GaAs buffer layer (1 μm thick), which is usually weakly n -type. Thus the photohole recombination centers, residual neutral donors d^0 , are very dilute and spread throughout the thick buffer layer. They are too far away from the source/drain channel to produce noticeable discrete jumps in current for single-photon events at $\lambda = 700$ nm. Nonetheless, the smooth photoconductance channel quantization steps are still observed at $\lambda = 700$ nm, as shown in Fig. 2(a).

The photoelectron plays a lesser role. It usually ends up in the channel, and then becomes swept away in the source and drain electrodes. Since those are ohmic contacts, they can continue to inject replacement electrons indefinitely. This is essentially the mechanism²² of secondary photoconductivity and photoconductive gain that is responsible for the single-photon sensitivity.

The conductance curve in Fig. 2(a) ends at the 2 conductance units ($2e^2/h$) plateau. Above this conductance level, the gate-induced and photoinduced conductance changes no longer match. The photoinduced conductance change tends to saturate above 2 conductance units ($2e^2/h$), after about 70 discrete photon conductance steps, but the gate-induced change continues to higher conductance. We attribute the saturation of the photoinduced conductance to saturation of the doping-induced trapping centers. Within the active area of 3×10^{-10} cm² there are 3.3×10^{11} carriers/cm² or only about 100 carriers, explaining the saturation in photoconductance. At a channel capacitance of ≈ 0.1 fF, the 70 charges produce about the same electric field as the gate voltage

change of $\Delta V_g = 0.2$ V that was required to reach the $2(2e^2/h)$ conductance plateau.

In this photoconductive single-photon detector, a photo-hole is trapped, producing a discrete change in source/drain channel conductance. If the photosensitive layer were strained, the light/heavy hole degeneracy would be lifted, and the hole spin degree of freedom might be a viable long-lived qubit. Strained hole spin coherence has been maintained²³ for about 100 ns in *p* Silicon. In *n*-type material however, the trapped holes are subject to electron/hole recombination. It is generally accepted²⁴ that a trapped photo-electron spin is the preferred qubit compared to a photohole spin. Electron traps may require artificial engineering, for example, they could be electron potential wells created by electrostatic gates above a heterointerface.

In addition to changing the sign of the trapped carrier, a further change may be needed to increase the quantum efficiency. Photoconductive detectors can inherently be quite efficient, since the photocarriers are produced by band-to-band

absorption in a direct band gap semiconductor. Nonetheless, it might be desirable in practice to incorporate the absorbing region into an optical cavity to make it a cavity-enhanced photodetector.

In principle, a photoconductive detector can store and detect an optically injected photocarrier charge, preserving its quantum mechanical spin information. This would safely prevent the charge measurement from disturbing the spin. We have demonstrated single photocarrier charge sensitivity, but we have used naturally occurring defect centers that are subject to carrier recombination. It remains yet to create an artificial potential well that would safely trap and store the spin.

We thank Hong Wen Jiang, James Chadi, and Mineo Saito for helpful discussions. The project is sponsored by the Defense Advanced Research Projects Agency and Army Research Office Nos. MDA972-99-1-0017 and DAAD19-00-1-0172.

*On leave from Fundamental Research Laboratories, NEC Corporation.

¹A. Yoshizawa and H. Tsuchida, *Jpn. J. Appl. Phys.* **40**, 200 (2001).

²G.A. Antypas and J. Edgecumbe, *Appl. Phys. Lett.* **26**, 371 (1974).

³C.H. Bennett *et al.*, *Phys. Rev. Lett.* **70**, 1895 (1993).

⁴R. Vrijen and E. Yablonovitch, *Physica E (Amsterdam)* **10**, 569 (2001).

⁵A.J. Shields *et al.*, *Appl. Phys. Lett.* **76**, 3673 (2000).

⁶S. Komiyama, O. Astafiev, V. Antonov, T. Kutsuwa, and H. Hirai, *Nature (London)* **403**, 405 (2000).

⁷B.J. van Wees *et al.*, *Phys. Rev. Lett.* **60**, 848 (1988).

⁸D.A. Wharam *et al.*, *J. Phys. C* **21**, L209 (1988).

⁹K.J. Thomas *et al.*, *Phys. Rev. Lett.* **77**, 135 (1996).

¹⁰C.-K. Wang and K.-F. Berggren, *Physica E (Amsterdam)* **2**, 964 (1998).

¹¹R.J. Nelson, *Appl. Phys. Lett.* **31**, 351 (1977).

¹²A. Kastalsky and J.C.M. Hwang, *Solid State Commun.* **51**, 317 (1984).

¹³H.P. Wei and D.C. Tsui, *Appl. Phys. Lett.* **45**, 666 (1984).

¹⁴D.V. Lang and R.A. Logan, *Phys. Rev. Lett.* **39**, 635 (1977).

¹⁵D.V. Lang, R.A. Logan, and M. Jaros, *Phys. Rev. B* **19**, 1015 (1979).

¹⁶D.J. Chadi and K.J. Chang, *Phys. Rev. Lett.* **61**, 873 (1988).

¹⁷D.J. Chadi and K.J. Chang, *Phys. Rev. B* **39**, 10 063 (1989).

¹⁸R.A. Linke, I. Redmond, T. Thio, and D.J. Chadi, *J. Appl. Phys.* **83**, 661 (1998).

¹⁹G. Brunthaler, K. Ploog, and W. Jantsch, *Phys. Rev. Lett.* **63**, 2276 (1989).

²⁰K.S. Ralls *et al.*, *Phys. Rev. Lett.* **52**, 228 (1984).

²¹It is now understood that DX^- is a donor ion that has captured an extra electron, thereby shifting to an interstitial site (Refs. 16 and 17). It has a negative- U property, preferring to take the electron from another donor in the reaction $2d^0 \rightarrow d^+ + DX^-$.

²²*Concepts in Photoconductivity and Allied Problems*, edited by A. Rose (Krieger, Huntington, New York, 1978).

²³G. Feher, J.C. Hensel, and E.A. Gere, *Phys. Rev. Lett.* **5**, 309 (1960).

²⁴D.D. Awschalom and J.M. Kikkawa, *Phys. Today* **52**(6), 33 (1999).